Science of Sintering, **48** (2016) 209-220

doi: 10.2298/SOS1602209T

UDK 531.3; 541.183

Microstructural Characterization and Adsorption Properties of Alkali-Activated Materials Based on Metakaolin

Katarina Trivunac[1*)], Ljiljana M. Kljajević[2], Snežana Nenadović[2], Jelena Gulicovski[2], Miljana Mirković[2], Biljana Babić[2], Slavica Stevanović[1]

[1)] Faculty of Technology and Metallurgy, Karnegijeva 4, University of Belgrade, Belgrade, Serbia

[2)] Institute of Nuclear Science ″Vinča″, P.O.Box 522, University of Belgrade, Belgrade, Serbia

Abstract:

The microstructural characterization and adsorption properties of metakaolin (MK) and alkali-activated metakaolin, known as geopolymer materials (GP) were investigated. The structure and properties of the metakaolin and obtained geopolymer were studied by X-ray diffraction (XRD), scanning electron microscopy (SEM) and Fourier transform infrared (FTIR) spectroscopy. Furthermore, based on the analysis of adsorption efficiency, microstructure and mineral structure, the difference between geopolymer and metakaolin on the performance of immobilizing heavy metals have been discussed. The kinetics of adsorption can be represented by pseudo-second order equation. The results of lead ions adsorption experiments were best fitted by Freundlich adsorption isotherm for both investigated adsorbents. The highest removal efficiencies of alkali-activated material based on metakaolin was found 97.5% at pH 4 and metakaolin removal efficiencies was found 92% at pH 5.5.

Keywords: *Metakaolin; Geopolymer; Heavy metal; Wastewater treatment; Adsorption kinetics*

1. Introduction

A large number of different methods are used for removal of heavy metals from wastewater, for example coagulation [1], precipitation, ion exchange [2], extraction, membrane filtration [3, 4]. As the tendency for methods in wastewater treatment is to be more efficient, inexpensive and environmentally responsible, adsorption on natural materials [5-7] or modified waste materials becomes relevant and the subject of many researches [8]. The influence of the structure of natural domestic materials (kaolin and diatomite) on the adsorption properties of lead were examined in the studies Nenadovic et al. [9, 10]. There is a worldwide tendency to use cheap materials as a potential sorbents [11, 12]. Among them, metakaolin and metakaolin-based geopolymers increasingly find applications. Metakaolin is a relatively complex material derived from a naturally occurring mineral and is usually produced by calcination of kaolin clays within a definite temperature range depending on the purity and crystallinity of the precursor clay [13-16]. Serbia has high-quality kaolin clay deposits at Aranđelovac and Kolubara basin, and thus good potential to produce metakaolin from them [10]. Geopolymers (alkali-activated metakaolin) are considered to be a group of

[*)] **Corresponding author**: trivunac@tmf.bg.ac.rs

modern aluminosilicate materials of composition and properties allowing their application in numerous new technologies [17]. In recent years, geopolymer materials have attracted much more attention due to their low density, low cost, low curing/hardening temperatures, environmentally friendly nature and excellent thermal stability at high temperatures [18-20]
The aim of this study is investigation of microstructure and adsorption properties of metakaolin and alkali-activated materials based on metakaolin - geopolymer as the considerably more economical materials for removal of the ionic lead pollution from industrial wastewater. A series of adsorption tests to investigate the influences of different parameters on the effectiveness of metakaolin and alkali-activated metakaolin - geopolymer on lead adsorption as a very toxic element were performed. It is known that lead ions in the heavy metal pollution are one of the important environmental problems in the aqueous system originated from industry. Additionally, the microstructural characterization and some chemical properties of the metakaolin and obtained geopolymer based on metakaolin were studied by X-ray diffraction (XRD), scanning electron microscopy (SEM) and Fourier transform infrared (FTIR) spectroscopy.

2. Experimental procedure

Metakaolin (MK) was prepared by calcining kaolinite at 750 °C for 3 h. The used kaolinite is high quality clay obtained from Rudovci, Lazarevac, Serbia. Physicochemical properties of kaolin were done in previous research Nenadovic et al [10]. Metakaolin and alkaline solution were mixed 10 min (solid/liquid = 0.85). The alkaline solution was mixed by sodium silicate (technical grade) and 16M NaOH (Sigma Aldrich analytical grade). The samples were cast into 25 mm diameter molds. The alkali-activated material- geopolymer (GP) was formed after sitting at room temperature for one day and at 50 °C for 2 days in a sample drying oven. Upon removal from the molds, the samples were crushed and sieved through sieve with hole of diameters of 355 μm. The contents of SiO_2 and Al_2O_3 were determined by conventional chemical analysis. The contents of SiO_2 were 55.32% and 47.98 % and, Al_2O_3 are 26.13 % and 17.40 % in metakaolin and geopolymer respectively. Samples of MK and GP were characterized by X-ray diffractometry (XRD) by using Ultima IV Rigaku diffractometer, equipped by Cu $K\alpha_{1,2}$ radiation, with generator voltage 40.0 kV and generator current 40.0 mA. The range of 10°-80° 2θ was used for all powders in a continuous scan mode with a scanning step size of 0.02° at scan rate of 10 °/min. The morphology and microstructure of the materials were studied by using SEM - JEOL JCM-5800 LV. The functional groups of MK and the GP were studied using FTIR spectroscopy a Perkin Elmer FT-IR spectrometer, Spectrum Two. The specific surface area, S_{BET}, pore size distribution (PSD) for the samples were calculated from the adsorption and desorption isotherms of N_2 and, were measured on samples, at -196°C, using the gravimetric McBain method. The particle size distribution was estimated by applying BJH method [21] to the desorption branch of isotherms while mesopore surface and micropore volume were estimated using the high resolution α_s plot method [22-24]. Micropore surface, S_{mic}, was calculated by subtracting S_{meso} from S_{BET}.

In this study a series of adsorption tests at room temperature to investigate the influences of different parameters on the effectiveness of MK and GP on lead adsorption were performed. The adsorbent was primarily heated in an oven at 100 ^oC for 16 hours and cooled in a desiccator before using it in the adsorption process. Solution of Pb(II) ion was prepared by dissolving lead nitrate in deionized water. The initial pH of the solutions was adjusted with HCl or NaOH to a desired value. After adsorption, the solution was filtered and the filtrate was analyzed for lead concentration by atomic absorption spectrophotometry (AAS Pye Unicam) at 217.0 nm. Different experimental parameters, such as pH, dosage of adsorbents, initial concentrations of the sample solution and contact time were tested to study their effects

on the removal of Pb(II) by the MK and GP. The removal efficiency, R, on metakaolin and geopolymer was calculated with equation (1):

$$R = \frac{c_0 - c_e}{c_0} 100 \quad (1),$$

where c_0 and c_e are the initial and equilibrium concentrations of lead ions (mg/L). The adsorption capacity (amount adsorbed per unit mass of adsorbent) q_e (mg/g) was calculated with equation (2):

$$q_e = \frac{(c_0 - c_e)V}{m} \quad (2),$$

where V represents volume of the solution and m is the mass of the adsorbent.

3. Results and Discussions

XRD patterns of metakaolin and alkali-activated material based on metakaolin - geopolymer are presented in Fig.1.

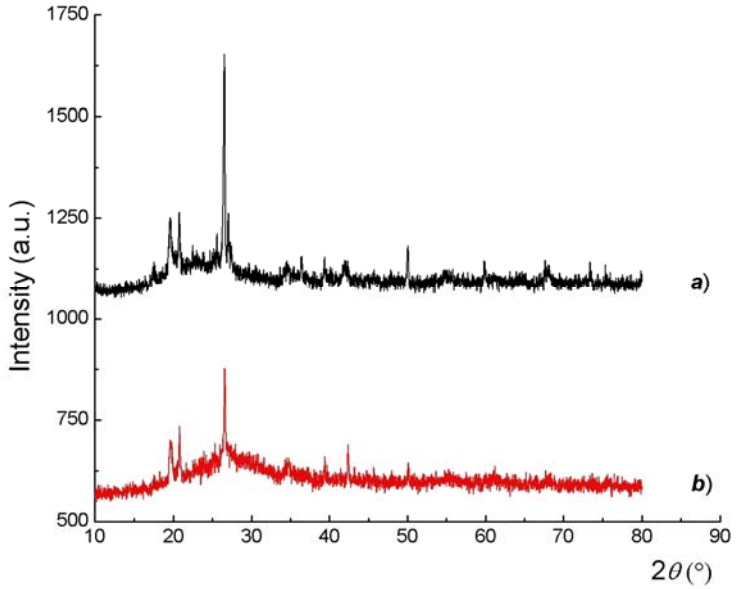

Fig. 1. XRD patterns of a) MK (metakaolin) and b) GP (geopolymer).

X-ray patterns prove that the part of SiO_2 originated from crystallic quartz (SiO_2,). A broad reflection centered at 2θ = 26.64° attribuTab. to the amorphous metakaolinite along with residual quartz (Fig 1). After dehydration process the kaolin loses its crystal structure and become mainly amorphous material. Similar behavior was commonly noted for geopolymers, with the proportion of the amorphous phase slightly higher compared to metakaolin. FTIR spectroscopy was used to characterize the metakaolin and alkali activated samples as illustrated in Fig. 2.

The analysis of FTIR spectrum of MK (Fig 2a) shows the strong bands of Si–Si stretching vibrations are present at 485 cm^{-1}. Bands at 793.9 cm^{-1} and 562.2 are a translational vibration band for Si-O-Al. The band at 804 cm^{-1} can be related to the change from octahedral coordination of Al^{3+} in kaolinite to tetrahedral coordination in metakaolinite. The shift of the peak of the GP was 1024.6 cm^{-1} compared to 1064 cm^{-1} for that of the MK indicated the chemical change and geopolymerization of NaOH-activated MK at elevated temperature. The bands observed at 1024.6 and 745 cm^{-1} represent the stretching bands of Si–O–Si groups and the deformation bands of Si–O respectively.

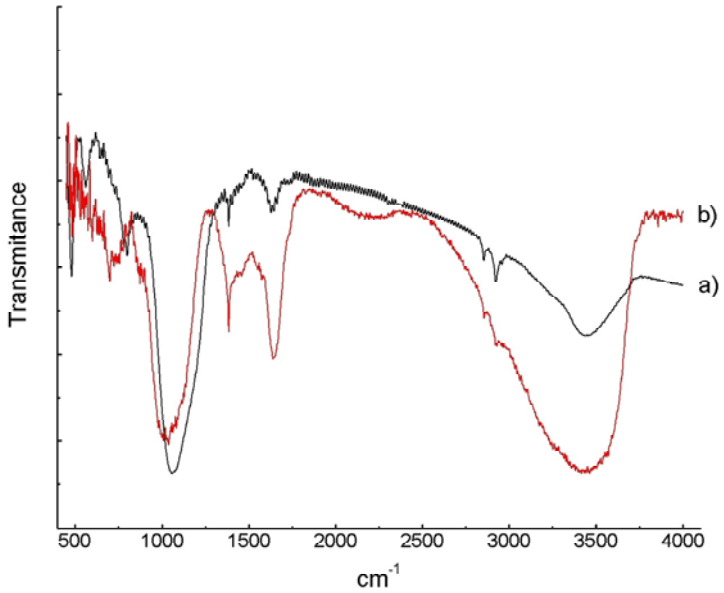

Fig. 2. FTIR spectrum of a) MK (metakaolin) and b) GP (geopolymer).

The analysis of spectrum of GP shows a broad band of spectrum observed at 3442.4 cm^{-1} signifying the O-H stretching vibrations of the H–O–H, Si–OH and Al–OH groups. The spectral band at 1641.4 cm^{-1} also represents the bending HOH bond of water molecules retained in the silica matrix. Microstructure of MK and GP powders are presented in Fig 3.

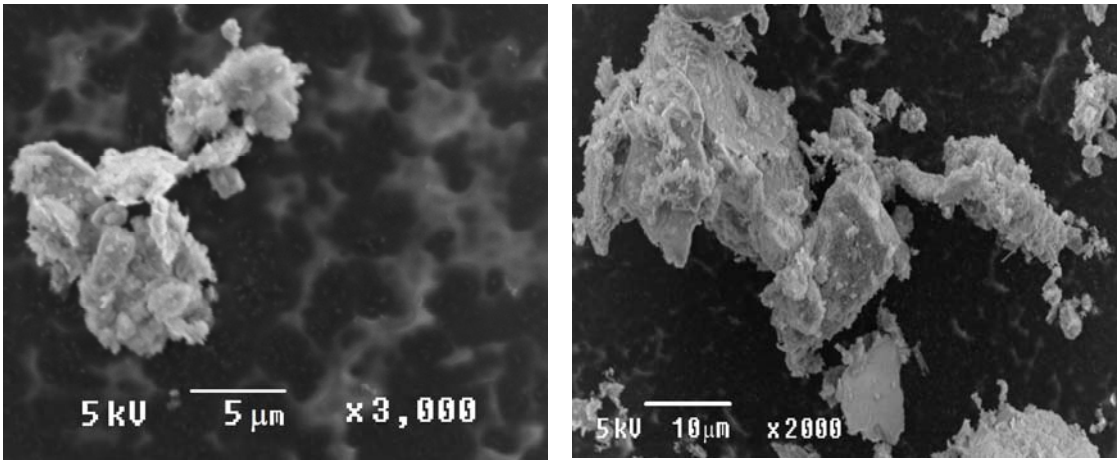

a) b)

Fig. 3. SEM micrographs of a) MK powder and b) GP sample after grinding.

Some of MK particles (Fig 3a) are platy in shape, but they have tendency to create higher agglomerate of circle shape. The process of calcination makes the particles less bulky and less hexagonally shaped, unlike the crystallized kaolinite crystals. Fig 3b shows the microstructure of a GP (after grinding) which are used for further process of adsorption. Geopolymer particles are different in shapes and size and show tendency to agglomerate as well as MK particles do. Some particles of GP tend to have polyhedral shape unlike MK circular like shape particles (this shape has minimum surface relative to the volume of the particles).

Nitrogen adsorption–desorption isotherms of MK and GP are presented in Fig. 4.

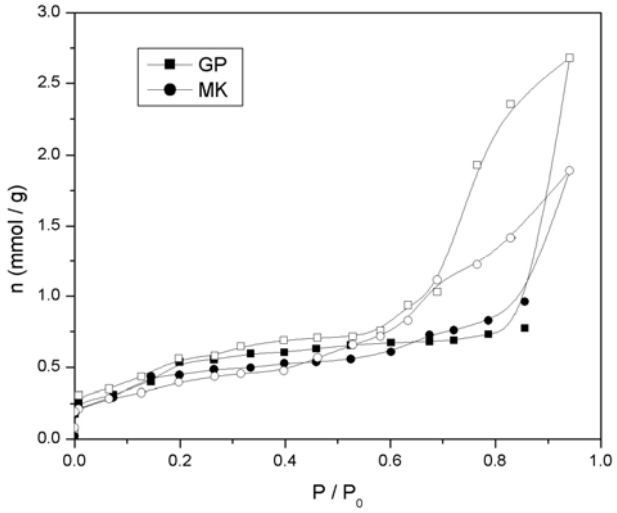

Fig. 4. Nitrogen adsorption (solid symbols) and desorption (open symbols) isotherms of GP and MK samples

The main feature of this type of isotherm is the hysteresis loop, which is associated with capillary condensation taking place in mesopores (pore size between 2 and 50 nm) [25]. In both samples, the shape of hysteresis loop is of type H2 which indicates a poorly defined shape of pores [24]. Pore size distribution (PSD) for GP and MK samples is shown in Fig. 5.

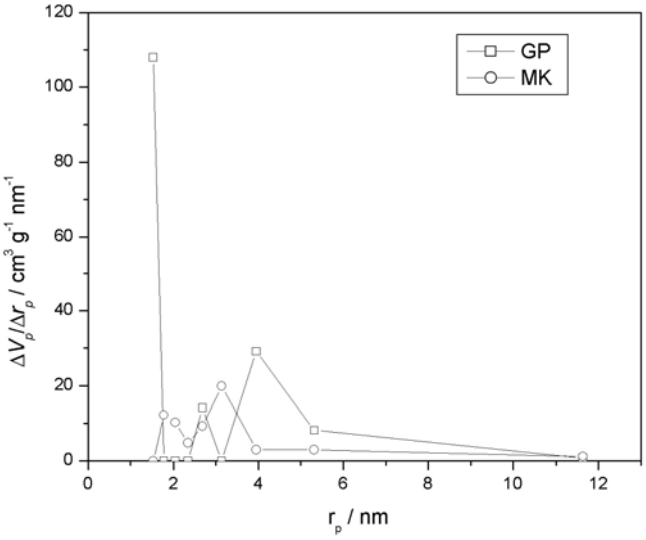

Fig. 5. Pore size distribution (PSD) for GP and MK samples.

GP sample has micro- and mesoporosity while MK has only mesopores. Mesopores are typical pores between geopolymer phases, while micropores exist within the gel network [24]. The formation of capillary pores is characteristic of cement systems, while their formation in GP is less distinct, because the gel takes up most of the space [26]. Specific surface area calculated by BET equation and for both samples is very similar, about 40 m^2/g for GP, and for MK 36 m^2/g (Tab. I).

Tab. I Porous properties of GP and MK samples.

Sample	S_{BET} (m^2/g)	S_{meso} (m^2/g)	S_{mic} (m^2/g)	V_{mic} (cm^3/g)
GP	40	13	27	0.014
MK	36	36	-	-

α_s plots, obtained on the basis of the standard nitrogen adsorption isotherm are shown in Fig. 6.

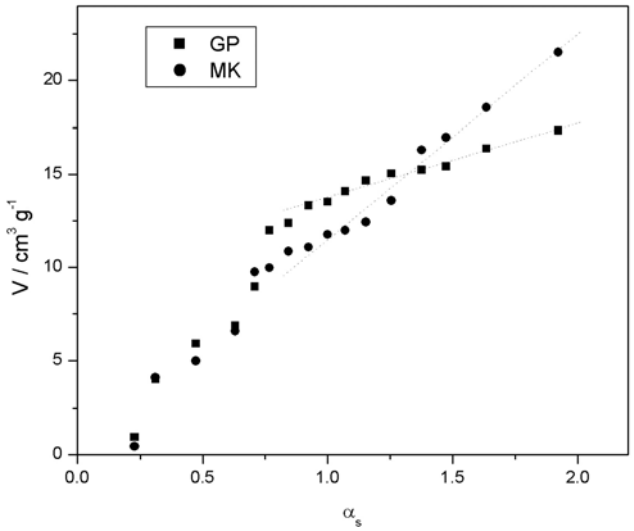

Fig. 6. α_S– plots for nitrogen adsorption isotherm of for metakaolin based geopolymer (GP) and metakaolin (MK) samples.

The straight line in the high α_s region gives a mesoporous surface area including the contribution of external surface, S_{meso}, determined by its slope, and micropore volume, V_{mic}, is given by the interception. Calculated porosity parameters (S_{meso}, S_{mic}, V_{mic}) are given in Tab. I.

3.1. Adsorption properties of metakaolin and alkali-activated metakaolin-geopolymer

Different operating parameters, such as pH, contact time, mass of adsorbent and initial concentration of solution were tested to study their effects on the removal of Pb(II) by the MK and GP and to determine adsorption properties of these materials.

3.1.1. Effects of pH and dosage of adsorbents

According to Fig. 7, optimum pH for adsorption is between 4-5 on GP and 5-6 on MK, which is consistent with the previous research works [27].

All other adsorption experiments were performed at pH of maximum removal efficiency, 4.5 for GP and 5.5 for MK. At higher pH, with decrease in concentration of H^+ ions, the competition between Pb^{2+} and H^+ ions for available positions on the negatively charged surface is smaller. Lead ions have precedence and efficiency is high. For pH values above 6.0, lead hydroxide begins to form resulting in the decrease of Pb(II) adsorption. At higher pH values the surface of the adsorbent is negatively charged as a result of deprotonation, and electrostatic repulsion decreases with increasing pH. At the Fig 8 influence of the adsorbent mass on the removal efficiency of MK and GP samples is showed.

At a low dosage of MK and GP, a large amount of adsorbate is available to be captured by the few available sites. At higher dosage of MK and GP i.e. of their solid particles, the number of binding sites available for the same volume of liquid increases, and thus, the total amount of lead ions that are removed increases. This increase is more pronounced for MK, although for the mass larger than 0.2 g, high R (90%) is achieved. In case of GP, high efficiency is achieved with a much smaller mass of adsorbent. Surface area

of GP is higher, possesses more available adsorption sites, and, as it was mentioned above, GP has micro and meso pores.

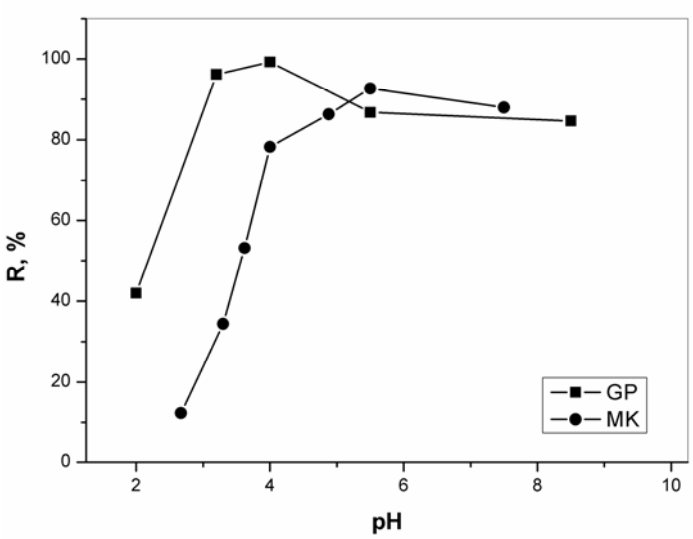

Fig. 7. Influence of pH value on removal efficiency of MK and GP (0.1 g MK/GP, 50 mg/dm^3 Pb, 60 minute).

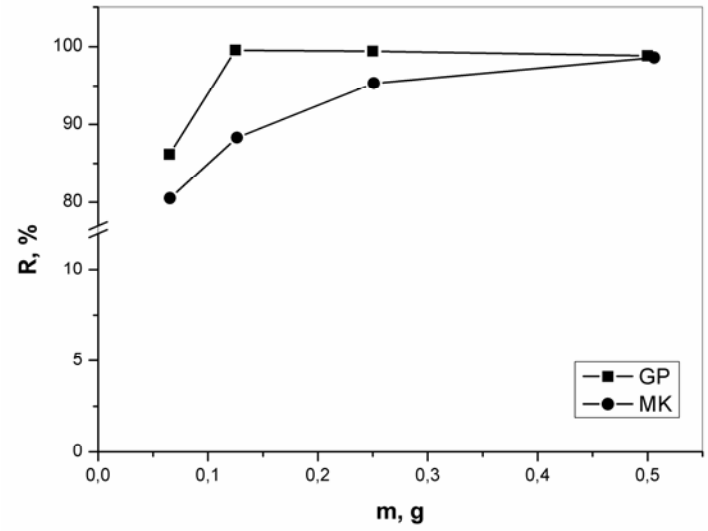

Fig. 8. Influence of adsorbent mass on removal efficiency of MK and GP (50 mg/dm^3 Pb, 60 minute, pH 4.5 for GP and 5.5 for MK).

3.1.2. Effects of contact time and initial lead concentration

Change of the efficiency to time is shown in Fig. 9.

It can be seen that the process occurs in two steps. In the first 10-30 minutes, adsorption is taking place rather quickly, achieving a steady state after approximately 45 minutes for MK and 20 minutes for GP. This initial step of fast adsorption corresponds to ions exchange in micropores and mesopores on the surfaces of GP and mesopores on the surface MK. After the initial step adsorption stay slow due to slower diffusion of ions into the layers of MK and into the channels of GP network. Fig 5 show that MK has only mesopores while geopolymer has micropores and mesopores. This is probably one of the reasons that the

efficiency of lead ions onto surface of MK is smaller than GP in both of steps of adsorption. The effects of initial lead ions concentration are shown in Fig 10.

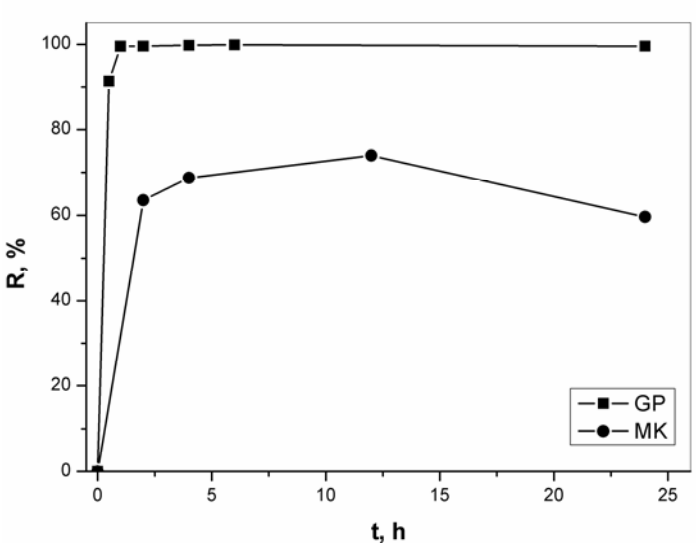

Fig. 9. Influence of contact time on removal efficiency of MK and GP (0.1 g MK/GP, 50 mg/dm^3 Pb, pH 4.5 for GP and 5.5 for MK).

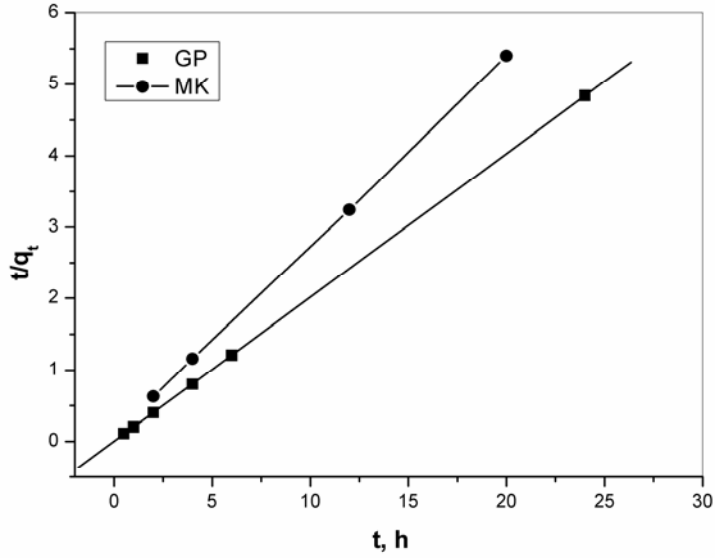

Fig. 10. Influence of initial concentration on removal efficiency of MK and GP (0.1 g MK/GP, 60 minute, pH 4.5 for GP and 5.5 for MK).

With the increase of concentration, the removal efficiency of MK is decreasing. Higher concentration of metal in the solution leads to the saturation of the adsorbent and the reduction of the free active contact surface causing a lower percentage of adsorption. The results for GP have different tendency. With the increase of concentration, no significant change in removal efficiency is observed. Due to changes in the structure of GP and the existence of network of Si-O groups that are available for binding, the number of adsorption positions increased. In the tested range of initial metal concentrations, the saturation of the adsorbent was not achieved and, therefore, the high R values were obtained in the experiments. Raising the initial metal ion concentration led to an increase in Pb(II) uptake by the used adsorbents [28].

3.2. Adsorption kinetics of investigated lead ions

The kinetics of lead (II) ion adsorption on both adsorbents was analyzed by linearized pseudo-first and pseudo-second kinetic models [27].
After integration and the application of boundary conditions t = 0 to t = t and $q_t = 0$ to $q_t = q_t$, the linear form of the pseudo-first order equation becomes:

$$\ln(q_e - q_t) = \ln q_e - K_1 t \quad (3)$$

where q_e and q_t are the adsorption capacities at equilibrium and at time t, respectively (mg/g) while K_1 is the rate constant for the pseudo-first order adsorption (L/min).

The integrated form of the pseudo-second order mechanism after applying the boundary conditions, t=0 to t=t and $q_t = 0$ to $q_t = q_t$ is given by:

$$\frac{t}{q_t} = \frac{1}{K_2 q_e^2} + \frac{t}{q_e} \quad (4)$$

where K_2 is the rate constant of pseudo-second order adsorption (g/mgmin).
The plot of t/q_t against t is represented in Fig. 11.

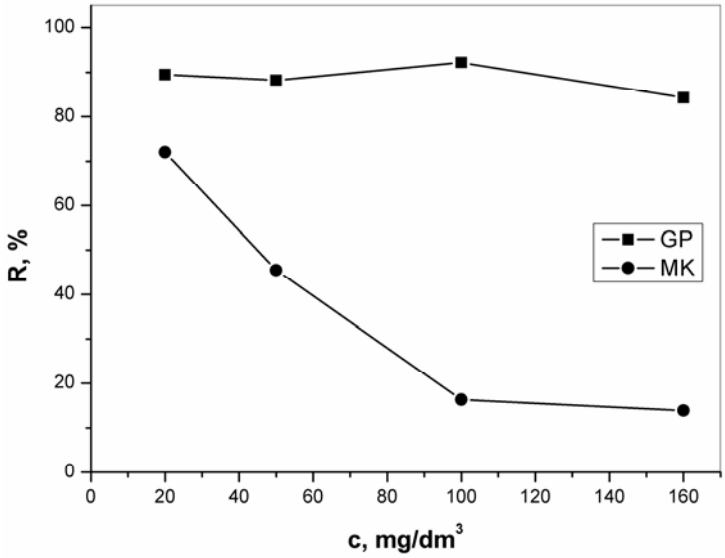

Fig. 11. Linearized pseudo-second order plots.

The plots gave a good fit to the experimental data for both investigated adsorbents. The calculated parameters, constants and corresponding linear regression correlation coefficients for tested kinetics models are presented in Tab. II.

Tab. II Kinetics model parameters.

Models	Parameters	Adsorbents	
		Metakaolin	Geopolymer
Pseudo-first order	K_1	0.176	0.00077
	q_e	0.809	0.809
	R^2	0.989	0.00037
Pseudo-second order	K_2	0.608	20.608
	q_e	3.830	4.963
	R^2	0.9999	1
	h	8.921	507.614

High correlation coefficient value for MK shows that pseudo-first kinetic model can be applied to predict the mechanism of adsorption onto this adsorbent. The results show that adsorption of Pb(II) ions on MK and GP are best described by the pseudo-second order kinetics. The higher R^2 values suggest that the adsorption of a metal by adsorbent may involve a chemical adsorption and its rate is limited by chemisorption. In some previous researches aimed at describing the adsorption of metals on various adsorbents [27, 29] pseudo-second order model has proven to be the most successful.

3.3. Adsorption isotherms

Among several isotherm models, experimental equilibrium data were fitted to the Langmuir, Freundlich, Temkin and Dubinin-Radushkevich model [27]. Equations describing each isotherm are presented in Tab. III, where, q_e is the adsorption capacities at equilibrium (mg/g); c_e is the equilibrium concentration in solution (mg/L); q_m is the maximum adsorption capacity (mg/g); K_L is the Langmuir constant (L/mg); F and n are empirical constants; ε is the potential of Polanyi, and is equal to RT $\ln(1+1/c_e)$; R is universal gas constant (J/Kmol); T is absolute temperature (K); K' is a constant related to the energy of adsorption (mol^2/KJ^2); b_T is Temkin isotherm constant; K_T is Temkin isotherm equilibrium binding constant (L/g).

Tab. III Isotherm adsorption models [27].

Adsorption isotherm	Equation	Linear form
Langmuir model	$q_e = q_m \frac{K_L c_e}{1 + K_L c_e}$	$\frac{1}{q_e} = \frac{1}{q_m K_L c_e} + \frac{1}{q_m}$
Freundlich model	$q_e = F c_e^{1/n}$	$\ln q_e = \ln F + \frac{1}{n} \ln c_e$
Dubinin-Radushkevich model	$q_e = q_m \exp\left(-K'\varepsilon^2\right)$	$\ln q_e = \ln q_m - K'\varepsilon^2$
Temkin model	$q_e = \frac{RT}{b} \ln\left(K_T c_e\right)$	$q_e = \frac{RT}{b_T} \ln K_T + \frac{RT}{b_T} \ln c_e$

Tab. IV Adsorption isotherm models parameters.

Models	Parameters	Adsorbents	
		Metakaolin	Geopolymer
Langmuir	q_m	15.69	16.49
	K_L	0.00718	0.054
	R^2	0.615	0.965
Freundlich	1/n	0.836	0.827
	K_F	0.218	0.873
	R^2	0.999	0.995
Temkin	B_T	0.155	2.273
	K_T	1.176	1.176
	R^2	0.284	0.967
Dubinin-Radushkevich	q_m	4.655	4.655
	K'	$1.4 \cdot 10^{-5}$	$6.72 \cdot 10^{-7}$
	R^2	0.814	0.854

Linear form of these equations was used for graphical plots of the experimental data. From the slope and the interception of the plots the models parameters were determined. Results are presented in Tab. 4. Adsorption of Pb(II) ions on MK is best fitted to Freundlich

isotherm model. This indicates adsorption in monolayer coverage but with heterogeneity of surface. Adsorption process on GP best described with three models since R^2 is greater then 0.96 for Langmuir, Freundlich and Temkin model. Best fiting is also with Freundlich isotherm model as it can be seen from Tab. IV. The results of the analysis indicate that the major factor for the improved adsorption of GP is the difference in the surface properties of the examined adsorbents.

4. Conclusion

The structure of metakaolin obtained using natural domestic clay raw appears disordered accordance to X-ray analysis. Similar behavior was commonly noted for geopolymers, with the proportion of the amorphous phase slightly higher compared to metakaolin. Phase evolution for metakaolin and geopolymer monitored by FTIR and, there are substantial changes in intensity, width and position of bands in the spectra of metakaolin and geopolymer. After activation with alkaline activating solution, the geopolymeric gel (spherical aggregates) formed, suggesting that the structure experiences growth. Geopolymer particles are different in shapes and size and show tendency to agglomerate as well as MK particles do. On the basis BET analysis was concluded that GP sample has micro- and mesoporosity while MK has only mesopores. Experimental data has shown that the both of these materials can successfully be used for the adsorption of lead ions from the solution. High values of the removal efficiency (>95%) was achieved due to the changes in the active surface and the internal structure of alkali-activated metakaolin as the number of potential positions for the binding of metal ions has increased. Adsorption processes can be described by Freundlich isotherm and kinetics model of pseudo second order. In both cases, a very good fitting of experimental and model data is obtained. Due to the high efficiency of adsorption, the easy availability of raw materials, low cost and energy consumption during synthesis, metakaolin and alkali-activated metakaolin – geopolymer could be widely used for the removal of lead ions from wastewater. These results are very good base for our further investigation of adsorption properties of used materials as adsorbent of the other heavy metals and many different pollutants of water.

Acknowledgment

This project was financially supported by the Serbian Ministry of Education, Science and Technological Development on projects III 45012 and 172007.

5. References

1. M. I. Ansari, A. Malik, Environ. Monit. Assess., 167 (2010) 163.
2. S. Rengaraj,. C.K. Joo, Y. Kim, J.Yi, J. Hazard Mater., 102 (2003) 275.
3. I. Korus, K. Loska, Desalination, 247 (2009) 390.
4. K.V. Trivunac, Z. Sekulic, S.M. Stevanovic, J. Serb. Chem. Soc., 77 (2012) 1670.
5. K.G. Bhattacharyya, S. Sen Gupta, Desalination, 272 (2011) 75.
6. A. Salem, R. Akbari Sene, Chem. Eng. J., 174 (2011) 628.
7. H. Liu, Sh Peng, L. Shu, T. Chen, T. Bao, R.L. Frost, Chemosphere, 91 (2013) 1546.
8. S. Wang, Y. Peng, Chem. Eng. J., 156 (2010) 24.

9. S. Nenadovic, M. Nenadovic, R. Kovacevic, Lj. Matovic, B. Matovic, Z. Jovanovic and J. Grbovic Novakovic, Sci. of Sintering, 41 (2009) 317.
10. S. S. Nenadovic, Lj. M. Kljajevic, M.T. Nenadovic, M. M. Mirkovic, S.B. Markovic, Z.Lj. Rakocevic, Environ. Earth. Sci., 73 (2015) 7677.
11. A. Bhatnagar, A.K. Minocha, Colloids. Surf. B, 76 (2010) 548.
12. S.Veli, B. Alyuz, J. Hazard. Mater., 149 (2007) 233.
13. J. Rocha, J, Klinowski, Angew. Chem. Int. Ed., 29 (1990) 554.
14. E. Badogiannis, G. Kakali, S. Tsivilis, J. Therm. Anal. Calorim., 81 (2005) 462.
15. M.L.Granizo, M.T. Blanco Varela, S. Martínez-Ramírez, J. Mater. Sci., 42 (2007) 2943.
16. B.R. Ilić, A.A.Mitrović, Lj. R. Miličić, Hem. ind., 64 (2010) 356.
17. J. Davidovits, Geopolymer Chemistry and Applications, Institut Géopolymère, Saint-Quentin, 2011.
18. A. Shvarzman, K. Kovler, G.S. Grader, G.E. Shter, Cem. Concr. Res., 33 (2003) 416.
19. V.F.F. Barbosa, K.J.D. MacKenzie, Mater. Lett., 57 (2003) 1482.
20. C.G. Papakonstantinou, P. Balaguru, R.E. Lyon, Compos. Part B-Eng., 32 (2001) 649.
21. E.P. Barret, L.G. Joyner, P.P. Halenda, J. Am. Chem. Soc., 73 (1951) 380.
22. K. Kaneko, C. Ishii, M. Ruike, H.H. Kuwabara, Carbon, 30 (1992)1088.
23. M. Kruk, M. Jaroniec, K.P. Gadakaree, J. Colloid. Interface. Sci., 192 (1997) 256.
24. K. Kaneko, C. Ishii, H.Kanoh, Y. Hanzawa, N. Setoyama, T. Suzuki, Adv. Colloid. Interface. Sci., 76-77 (1998) 320.
25. K.S.W. Sing, Pure Appl. Chem., 54 (1982) 2218.
26. Y. Ma, J. Hu , G.Ye, Fuel, 104 (2013) 780.
27. A.O. Dada, A.P. Olalekan, A.M.Olatunya, O. Dada, J. Appl. Chem., 3 (2012) 45.
28. Z. Melichová, A. Ľuptáková, Desalin. Water Treat., 57 (2016) 5025.
29. A. Sari, M. Tuzen, Appl. Clay Sci., 88–89 (2014) 72.

Садржај: *У раду су карактерисана микроструктурна и адсорпциона својства метакаолина (МК) и алкално-активираног метакаолина, познатог као геополимер (ГП). Структура и својства метакаолина и добијеног геополимера су изучаване применом рендгенске дифракције (XRD), скенирајуће електронске микроскопије (SEM) и инфрацрвене спектроскопије са Фуријеовом трансформацијом (FTIR). Разлика у имобилизацији тешких метала разматрана је на основу ефикасности адсорпције, микроструктуре и минералне структуре геополимера и метакаолина. Кинетика адсорпције може се представити једначином псеудо-другог реда. За оба испитивана адсорбенса резултати адсорпције јона олова су најбоље фитовани Фројндлиховом адсорпционом изотермом. Алкално-активирани материјал на бази метакаолина је показао највећу ефикасност адсорпције око 97,5% на pH 4, а метакаолин 92 % на pH 5.5.*

Кључне речи: *Метакаолин; геополимер; тешки метали; пречишћавање отпадних вода; кинетика адсорпције.*